

# Aligned microribbon-like hydrogels for guiding three-dimensional smooth muscle tissue regeneration

Soah Lee,<sup>1</sup> Xinming Tong,<sup>2</sup> Li-Hsin Han,<sup>2</sup> Anthony Behn,<sup>2</sup> Fan Yang<sup>1,2,3</sup>

<sup>1</sup>Department of Materials Science and Engineering, Stanford University, Stanford, California 94305

<sup>2</sup>Department of Orthopaedic Surgery, Stanford University, Stanford, California 94305

<sup>3</sup>Department of Bioengineering, Stanford University, Stanford, California 94305

Received 21 October 2015; revised 12 January 2016; accepted 19 January 2016

Published online 00 Month 2016 in Wiley Online Library (wileyonlinelibrary.com). DOI: 10.1002/jbm.a.35662

**Abstract:** Smooth muscle tissue is characterized by aligned structures, which is critical for its contractile functions. Smooth muscle injury is common and can be caused by various diseases and degenerative processes, and there remains a strong need to develop effective therapies for smooth muscle tissue regeneration with restored structures. To guide cell alignment, previously cells were cultured on 2D nano/microgrooved substrates, but such method is limited to fabricating 2D aligned cell sheets only. Alternatively, aligned electrospun nanofiber has been employed as 3D scaffold for cell alignment, but cells can only be seeded post fabrication, and nanoporosity of electrospun fiber meshes often leads to poor cell distribution. To overcome these limitations, we report aligned gelatin-based microribbons ( $\mu$ RBs) as macroporous hydrogels for guiding smooth muscle alignment in 3D. We developed aligned  $\mu$ RB-like hydrogels using wet spinning, which allows easy fabrication of tissue-scale (cm) macroporous matrices with alignment

and supports direct cell encapsulation. The macroporosity within  $\mu$ RB-based hydrogels facilitated cell proliferation, new matrix deposition, and nutrient diffusion. In aligned  $\mu$ RB scaffold, smooth muscle cells showed high viability, rapid adhesion, and alignment following  $\mu$ RB direction. Aligned  $\mu$ RB scaffolds supported retention of smooth muscle contractile phenotype, and accelerated uniaxial deposition of new matrix (collagen I/IV) along the  $\mu$ RB. In contrast, cells encapsulated in conventional gelatin hydrogels remained round with matrix deposition limited to pericellular regions only. We envision such aligned  $\mu$ RB scaffold can be broadly applicable in growing other anisotropic tissues including tendon, nerves and blood vessel. © 2016 Wiley Periodicals, Inc. *J Biomed Mater Res Part A*: 00A:000–000, 2016.

**Key Words:** smooth muscle, three-dimensional, alignment, hydrogels, macroporous

---

**How to cite this article:** Lee S, Tong X, Han L-H, Behn A, Yang F. 2016. Aligned microribbon-like hydrogels for guiding three-dimensional smooth muscle tissue regeneration. *J Biomed Mater Res Part A* 2015:00A:000–000.

---

## INTRODUCTION

Smooth muscle tissue comprises the wall of many hollow organs in our body such as blood vessels, gastrointestinal tracts, urinary bladder, reproductive tracts, respiratory tracts, and so forth.<sup>1–5</sup> Smooth muscle tissue involuntarily contracts and relaxes to control specific organ functions such as regulating blood flow, mixing/transporting contents in stomach, storing/voiding urine, and serving a specialized contractile activity during pregnancy and childbirth. Smooth muscle tissue is composed of thin-elongated smooth muscle cells that lie parallel to one another in one direction for its contractile

function. During injury, smooth muscle cells undergo dedifferentiation or phenotypic alteration from contractile to synthetic phenotype, which contributes to the pathogenesis of many diseases including atherosclerosis, asthma, urinary incontinence, and so forth.<sup>1,6,7</sup> To treat diseases caused by smooth muscle loss, cell-based therapy has emerged as a promising therapeutic option by delivering cells to the target site to promote smooth muscle regeneration. A few studies have explored the feasibility of delivering smooth muscle cells or stem cells from adipose or bone marrow for smooth muscle repair.<sup>8–10</sup> However, these strategies do not support cell

Additional Supporting Information may be found in the online version of this article.

Winner of the Young Investigator Award of the Society for Biomaterials (USA) for 2016, 10th World Biomaterials Congress, Montreal QC, Canada, May 17–22, 2016.

**Correspondence to:** Fan Yang; Departments of Orthopaedic Surgery and Bioengineering, 300 Pasteur Dr., Edwards R105, Stanford University School of Medicine, Stanford, CA 94305, USA; e-mail: fanyang@stanford.edu

Contract grant sponsor: NIH R01DE02,4772, California Institute for Regenerative Medicine Tools and Technologies Development Grant; contract grant number: RT3–07,804

Contract grant sponsor: California Institute for Regenerative Medicine Early Translational III Grant; contract grant number: TR3–05,569

Contract grant sponsor: Bio-X Interdisciplinary Initiatives Program Grant, National Science Foundation CAREER award program; contract grant number: CBET-13,51 289

Contract grant sponsor: Stanford Chem-H Institute

alignment and tissue formation with biomimetic aligned tissue structures, which is critical for the contractile function of smooth muscle tissues.

To guide cell alignment *in vitro*, several strategies have been developed including the use of aligned substrate,<sup>11</sup> and electrospun fiber meshes.<sup>12–15</sup> Using thermoresponsive nanogrooved substratum and gel casting method, one group has reported effective formation of aligned cell sheets, which can be further stacked to form dense tissues with aligned structure.<sup>11</sup> However, stacking single layers of aligned cell sheets is very challenging and labor-intensive, and do not facilitate scaling up for fabricating tissue scale grafts. Furthermore, densely packed cell sheets poses a great challenge for cell survival due to lack of diffusion,<sup>16</sup> and lacks porosity, that is, desirable for cell infiltration, proliferation, and new matrix deposition. An alternative strategy for achieving cell alignment utilizes aligned electrospun fiber meshes composed of biodegradable polymers such as poly(lactic-co-glycolic acid) and poly( $\epsilon$ -caprolactone).<sup>12–15</sup> Since electrospinning process is not cell friendly, cells can only be seeded after the scaffold fabrication. While electrospun fiber meshes provide a 3D scaffold with aligned cues, cell penetration is challenging due to the nanoporosity, and cell infiltration is typically limited to within  $\sim 100$  s of  $\mu\text{m}$  from the scaffold surface with inhomogeneous cell distribution.<sup>12,14,15,17</sup> As such, there remains a critical need to develop novel strategies that would support cell alignment in 3D.

An ideal scaffold for smooth muscle repair should meet the following criteria: guides cell alignment and tissue formation in 3D, supports direct cell encapsulation, can be fabricated easily in tissue scale (cm), and has macroporosity. Macroporosity is important to enhance diffusion, cell survival, and accelerate new matrix deposition without delay. Ability to directly encapsulate cells is critical for fabricating tissue-scale cell-laden tissues with desirable homogeneity. Recently, our group has reported gelatin-based microribbon ( $\mu\text{RB}$ )-like hydrogels that can crosslink into a macroporous scaffold while supporting direct and homogeneous cell encapsulation.<sup>18</sup> The previously reported  $\mu\text{RB}$  scaffold is randomly intercrosslinked without alignment, but satisfies two desirable scaffold requirements for smooth muscle repair: macroporosity and direct cell encapsulation. The goal of this study is to develop a method to align the  $\mu\text{RB}$ s for guiding smooth muscle cell alignment in 3D, and validating the potential of aligned  $\mu\text{RB}$ -like hydrogels for supporting smooth muscle cell phenotype retention and matrix deposition *in vitro*. Aligned  $\mu\text{RB}$ s were fabricated by wet-spinning gelatin into a rotating collector. To evaluate the potential of aligned  $\mu\text{RB}$  scaffold for smooth muscle repair, human bladder-derived smooth muscle cells (SMCs) were encapsulated into aligned  $\mu\text{RB}$ -like hydrogels and cultured *in vitro* for up to 28 days. SMCs were also encapsulated in conventional nanoporous gelatin hydrogels without alignment cues as a control. Scaffold morphology was examined using scanning electron microscopy. Outcome analysis included cell viability, morphology, protein expression, new matrix deposition, and mechanical testing.

## EXPERIMENTAL

### Synthesis and fabrication of aligned gelatin-based $\mu\text{RB}$ s

Aligned gelatin-based  $\mu\text{RB}$ s were fabricated by modifying our previously reported  $\mu\text{RB}$  synthesis method.<sup>18</sup> Briefly, type-A gelatin (Gela, Sigma-Aldrich, St. Louis, MO) was dissolved in dimethyl sulfoxide (DMSO, Sigma-Aldrich) at 15% (w/w) concentration, and stirred at 350 rpm for 3 h, followed by stirring at 125 rpm overnight on hot plate (60°C) to achieve viscous Gela/DMSO solution. The viscous solution was then transferred into 30-mL syringe and wet-spun into an ethanol bath (1.8 L) at constant flow rate (3 mL/h) controlled by syringe pump (kdScientific, 78–8200, Holliston, MA). In the ethanol bath, the Gela solution precipitated into microfibers and as formed microfibers were collected in aligned manner around a rotating magnet-containing U-shaped collector (750 rpm) located in the bottom of the ethanol bath. Each aligned  $\mu\text{RB}$  scaffold was fabricated using 75  $\mu\text{L}$  of gelatin solution, and then a new collector was used to collect a new scaffold. The collected microfibers were kept on U-shaped holder to maintain alignment, and subsequently transferred to acetone for 1 h to induce collapse into  $\mu\text{RB}$  shape. To functionalize 15% of primary amine groups of gelatin into photocrosslinkable methacrylate groups,  $\mu\text{RB}$ s were reacted with a 0.1 mM solution of methacrylic acid N-hydroxysuccinimide ester (Sigma Aldrich) in methanol overnight. To retain  $\mu\text{RB}$  morphology, methacrylate-coated  $\mu\text{RB}$ s were transferred into a 0.1 mM solution of glutaric dialdehyde (Sigma Aldrich) in methanol and were internally crosslinked for 24 h. The unreacted aldehyde in the cross-linked  $\mu\text{RB}$ s were quenched using 1 mM solution of L-lysine hydrochloride (Sigma Aldrich) in PBS at 37°C overnight. After quenching, the aligned  $\mu\text{RB}$ s were washed using Ultrasterile water (Invitrogen, Grand Island, NY) at 37°C for 1 h and the washing was repeated with fresh Ultrasterile water three times. After vigorous washing, the aligned  $\mu\text{RB}$ s were lyophilized on the U-shape holder and stored at  $-20^\circ\text{C}$  until use.

### Gelatin methacrylate synthesis

Gelatin methacrylate (MA) was synthesized using previously reported method.<sup>19</sup> Briefly, 5 g of gelatin type B (Sigma Aldrich) was added in 50 mL of deionized (DI) water with stirring in a water bath on hot plate (325 rpm, 37°C) until gelatin completely dissolved. Then, 5 mL of methacrylic anhydride (Sigma Aldrich) was added to the gelatin solution and was stirred for 1 h. The gelatin–MA solution was added drop by drop into stirring acetone to be precipitated. The gelatin–MA precipitate was transferred into warm DI water to be redissolved, followed by dialysis against fresh DI water for 2 days. The dialyzed gelatin–MA solution was filtered, freeze-dried, and stored at  $-20^\circ\text{C}$  until use.

### Cell culture

Human primary bladder-derived smooth muscle cells (SMCs, Lonza, Allendale, NJ) were cultured according to manufacturer's guideline. Briefly, SMCs were plated at 3500 cells/cm<sup>2</sup> and expanded in smooth muscle growth media (SMGM, Lonza, CC-3182) until 80% confluency. SMCs were passaged

every 5–7 days using trypsin/EDTA (Invitrogen) and used at passage five for all experiments.

### Cell encapsulation

For aligned  $\mu$ RB groups, 10% (w/v)  $\mu$ RB was prepared with cell density of 5 M/mL. First, 20 mg of freeze-dried  $\mu$ RBs with U-shape holder were hydrated with 140  $\mu$ L of SMGMs with photoinitiator Irgacure 2959 (0.05% (w/v), Ciba Specialty Chemistry, Basel, Switzerland). After  $\mu$ RBs were fully hydrated, the remaining 60  $\mu$ L of Irgacure-containing SMGM containing 1M cells was pipetted at different locations and well-mixed before crosslinking. After mixing well to ensure homogeneous cell distribution, the aligned  $\mu$ RB scaffolds were exposed to UV light (365 nm, 4 mW/cm<sup>2</sup>, 5 min) for crosslinking. For cell encapsulation in conventional gelatin hydrogel as a control group, gelatin–MA powder was dissolved in Irgacure-containing SMGM (0.05% (w/v)) and mixed with SMCs to achieve 6% (w/v) polymer concentration and cell density of 10 M/mL. For each hydrogel sample, 25  $\mu$ L of the hydrogel precursor solution was loaded into cylindrical mold (1 mm in height, 5 mm in diameter) and was exposed to UV (365 nm, 4 mW/cm<sup>2</sup>, 5 min) to induce gelation.

### Cell viability

LIVE/DEAD<sup>®</sup> Viability/Cytotoxicity Kit, for mammalian cells (ThermoFisher Scientific, L-3224) was used to evaluate cell viability. Briefly, dye solution was prepared by diluting calcein AM (for live cells) and ethidium homodimer-1 (for dead cells) in SMGM at a final concentration of 2 and 4  $\mu$ M, respectively. Aligned  $\mu$ RB scaffolds and hydrogel scaffolds were incubated with the dye solution for 30 min on 3D rocker at 37°C. Live/dead cells were imaged using fluorescent microscope, and the images were colored using Fiji software.

### IMMUNOSTAINING

Cells were fixed by incubating with 4% paraformaldehyde/PBS for 1 h at room temperature, washed with washing buffer (0.1% Tween-20/PBS) for 1 h once, and washed/permeabilized with 0.1% Triton X-100/PBS for 1 h at room temperature twice. Cells were blocked with a blocking buffer (3% BSA/2% goat serum/PBS) for 1 h at room temperature. Cells were incubated with primary antibodies/blocking buffer (mouse smooth muscle myosin heavy chain (SM-MHC), Abcam ab683, 1:50; rabbit collagen I, Abcam ab3,4710, 1:100; rabbit collagen IV, Abcam ab6,586, 1:100) overnight at 4°C on shaker. Cells were washed with washing buffer for 1 h at room temperature three times, then incubated with secondary antibodies/Hoeschst dye/blocking buffer (Alexa 488 goat-antimouse, Invitrogen A1,1001, 1:300; rhodamine goat-antirabbit, Millipore AP132, 1:300; Hoeschst dye, Cell Signaling Technology 4,082S, 2  $\mu$ g/mL) for 1 h at room temperature on shaker. For cytoskeletal staining, cells were incubated with Rhodamine-phalloidin (Sigma P1951, 1:100 in blocking buffer) for 1 h at room temperature. Cells were again washed with washing buffer for 1 h three times, followed by imaging using confocal microscope (20 $\times$  oil immersion, Leica SP8 confocal system). Images were colored and overlaid using Fiji software.

### Tensile testing

Tensile testing of aligned  $\mu$ RB hydrogels was performed using an Instron 5944 materials testing system (Instron Corporation, Norwood, MA) fitted with a 100 N load cell. By the end of 28 day of culture, aligned  $\mu$ RBs were taken out from the U-shape holder and the  $\mu$ RB loops were inserted over horizontally aligned shafts (3 mm diameter) secured in the upper and lower grips. While under a preload of 5 mN, scaffold cross-sectional area and initial length were recorded with digital calipers and the test machine's position readout, respectively. Scaffolds were pulled at a rate of 1% strain/second to failure. Load and displacement data were recorded at 100 Hz. The tensile modulus was determined from a linear curve fit of the stress versus strain curve from 40–60% strain.

### Statistical analysis

Data are presented as mean  $\pm$  standard deviation ( $n = 3$ ). Unpaired Student's *t* test was used for between-group comparisons. *p* values less than 0.05 were considered statistically significant.

## RESULTS

### Fabrication and characterization of aligned $\mu$ RBs with tunable width

To fabricate  $\mu$ RB-like hydrogels into aligned structures, gelatin solution was wet-spun into microfibers and collected around a rotating U-shaped holder in ethanol to induce alignment [Fig. 1(A)]. The collected gelatin microfibers were then flattened into  $\mu$ RBs by transferring into acetone and internally crosslinked using aldehyde to maintain  $\mu$ RB shape. The  $\mu$ RB surface was modified with methacrylate groups to allow further intercrosslinking. Upon exposure to light (365 nm, 4 mW/cm<sup>2</sup>, 5 min), aligned methacrylated  $\mu$ RBs [10% (w/v)] intercrosslinked into hydrogels with retained alignment cues [Fig. 1(B)].

Scanning electron microscopy confirmed alignment of  $\mu$ RBs and presence of macroporosity [Fig. 1(C,D)]. The width of individual  $\mu$ RB was also tunable by varying injection rate of gelatin solution (3–10 mL/h), which yielded  $\mu$ RB with width ranging from 46 to 122  $\mu$ m [Fig. 1(C–E)].

### Aligned $\mu$ RB supported 3D cell encapsulation and alignment

To examine effects of macroporosity and alignment cue of  $\mu$ RB scaffolds on cell alignment, human bladder-derived smooth muscle cells (SMCs) were chosen as a model cell type. For  $\mu$ RB group,  $\mu$ RBs with 46  $\mu$ m width were used given its ability to guide better cell alignment than wider  $\mu$ RBs based on our optimization study (Supporting Information Fig. S1). As a control, cells were also encapsulated in conventional gelatin hydrogels, which was nanoporous without alignment cue.<sup>20</sup> Upon mixing with SMCs and exposed to light, both gelatin  $\mu$ RBs and conventional gelatin–MA precursor solution crosslinked successfully and formed cell-laden scaffolds with homogeneous cell distribution [Fig. 2(A)]. Cell viability was high in both  $\mu$ RB and gelatin–MA hydrogels 24 h after the encapsulation. However, distinct cell morphology was observed in  $\mu$ RB compared with gelatin–MA hydrogels [Fig. 2(B)]. Only  $\mu$ RB group led to fast

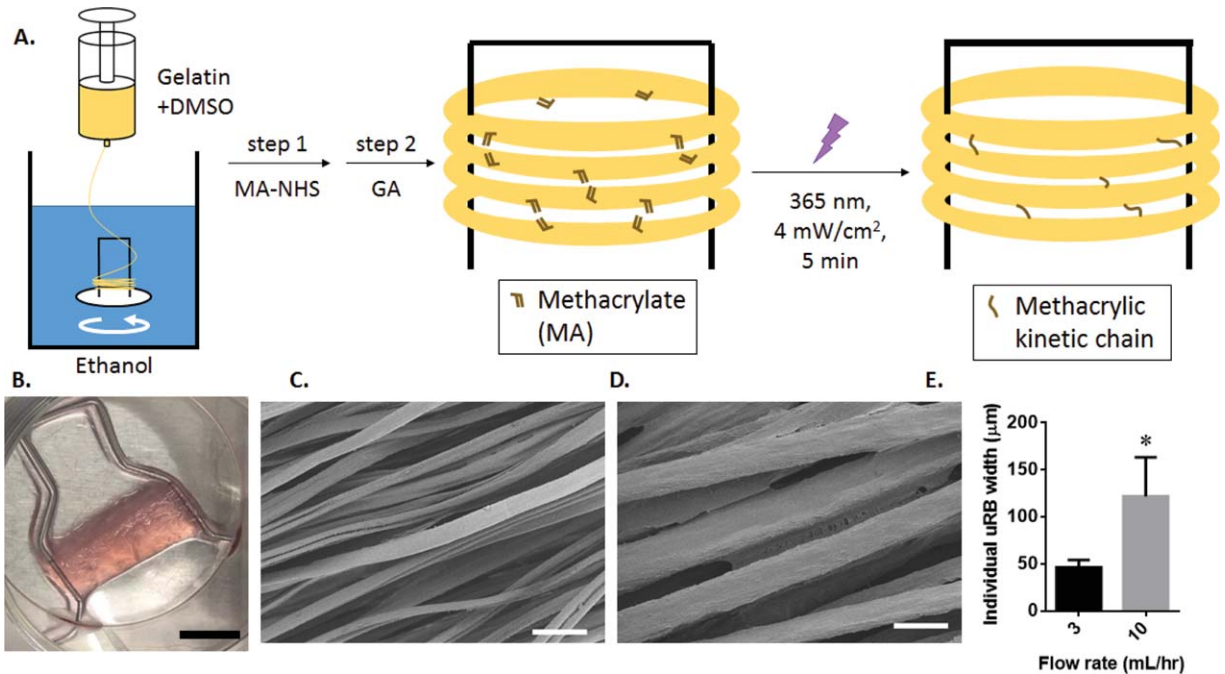


**FIGURE 1.** (A) Schematic of fabrication process of aligned microribbon ( $\mu$ RB) hydrogels. MA-NHS: methacrylic acid *N*-hydroxysuccinimide ester, GA: glutaric dialdehyde. (B) A photograph of cell-laden aligned  $\mu$ RB hydrogels on a U-shape holder after cell encapsulation (scale bar: 1 cm). (C, D) Scanning electron microscopy (SEM) images of aligned  $\mu$ RB hydrogels with tunable width fabricated by varying ejection rate of gelatin solution during wet-spinning process (C: 3 mL/h, D: 10 mL/h, scale bar: 200  $\mu$ m). (E) Quantification of  $\mu$ RB width from SEM images ( $n = 20$ ,  $*p < 0.05$ ).

cell adhesion and spreading, whereas cells remained round in gelatin–MA hydrogel group. Next, we evaluated cell morphology and alignment over time by immunostaining of F-actin, a cytoskeletal protein, at days 7 and 21. SMCs showed uniform alignment along the direction of  $\mu$ RBs at day 7, which persisted at day 21 [Fig. 2(C,D)]. In contrast, cells remained entrapped and round in gelatin–MA hydrogels up to 21 days.

#### Aligned $\mu$ RBs supported SMCs to retain contractile phenotype and guided alignment of newly deposited matrix proteins

The contractile phenotype of smooth muscle cells is crucial for its contractile function. We next examined whether aligned  $\mu$ RBs can support SMC cell to maintain contractile phenotype during 3D culture. Immunostaining for smooth muscle myosin heavy chain (MHC) confirmed that SMCs retained their contractile phenotype >21 days of culture in  $\mu$ RB scaffolds [Fig. 3(A,B)]. While MHC expression was observed in both  $\mu$ RB and gelatin–MA hydrogels, MHC organization was different between two groups. To study the effects of macroporosity and alignment cue of  $\mu$ RB scaffold on newly deposited extracellular matrix proteins, smooth muscle tissue abundant matrix proteins (Col I, Col IV) were stained at day 21 [Fig. 3(C,D)]. Importantly,  $\mu$ RBs guided the collagen deposition to align along  $\mu$ RBs, which mimics native smooth muscle morphology. In contrast, alignment of newly deposited collagen was not observed in gelatin–MA hydrogels, and the collagen deposition was only restricted to pericellular regions.

#### Cellular deposited extracellular matrix contributed to increase in tensile modulus

Since smooth muscle tissue plays an important role in relaxation/contraction, we next assessed the tensile strength of aligned  $\mu$ RB scaffolds using uniaxial tensile test [Fig. 4(A,B)]. At day 0 (D0), acellular  $\mu$ RB scaffold demonstrated that it can be stretched up to 200% strain and withstand maximum tensile stress of 75 kPa [Fig. 4(C)]. Calculated tensile modulus of D0 acellular  $\mu$ RB scaffold was 48 kPa [Fig. 4(D)]. After 28 days of culture, maximum tensile strain, maximum tensile stress, as well as tensile modulus of acellular  $\mu$ RB scaffold significantly decreased to 90%, 2, 2 kPa, respectively [Fig. 4(C,D)]. While maximum tensile stress and tensile modulus of cell-laden  $\mu$ RB scaffold also decreased, they were three times higher than those of acellular one, 6 and 7 kPa, respectively. Maximum tensile strain of cell-laden  $\mu$ RB scaffold was comparable to that of acellular  $\mu$ RB scaffold (85%) [Fig. 4(C,D)].

#### DISCUSSION

Many tissue types in human body is characterized by aligned morphology including muscles, tendons, nerves, and so forth. Recreating tissues with biomimetic alignment is critical for restoring the desirable tissue structures and functions. Towards this goal, several biomaterials platforms have been developed to guide cell alignment including culturing cells on nanogrooved substrates and electrospun nanofibers with alignment cues. These methods allow effective formation of aligned cells as a monolayer 2D, however, one of the biggest limitation is that they are not effective for

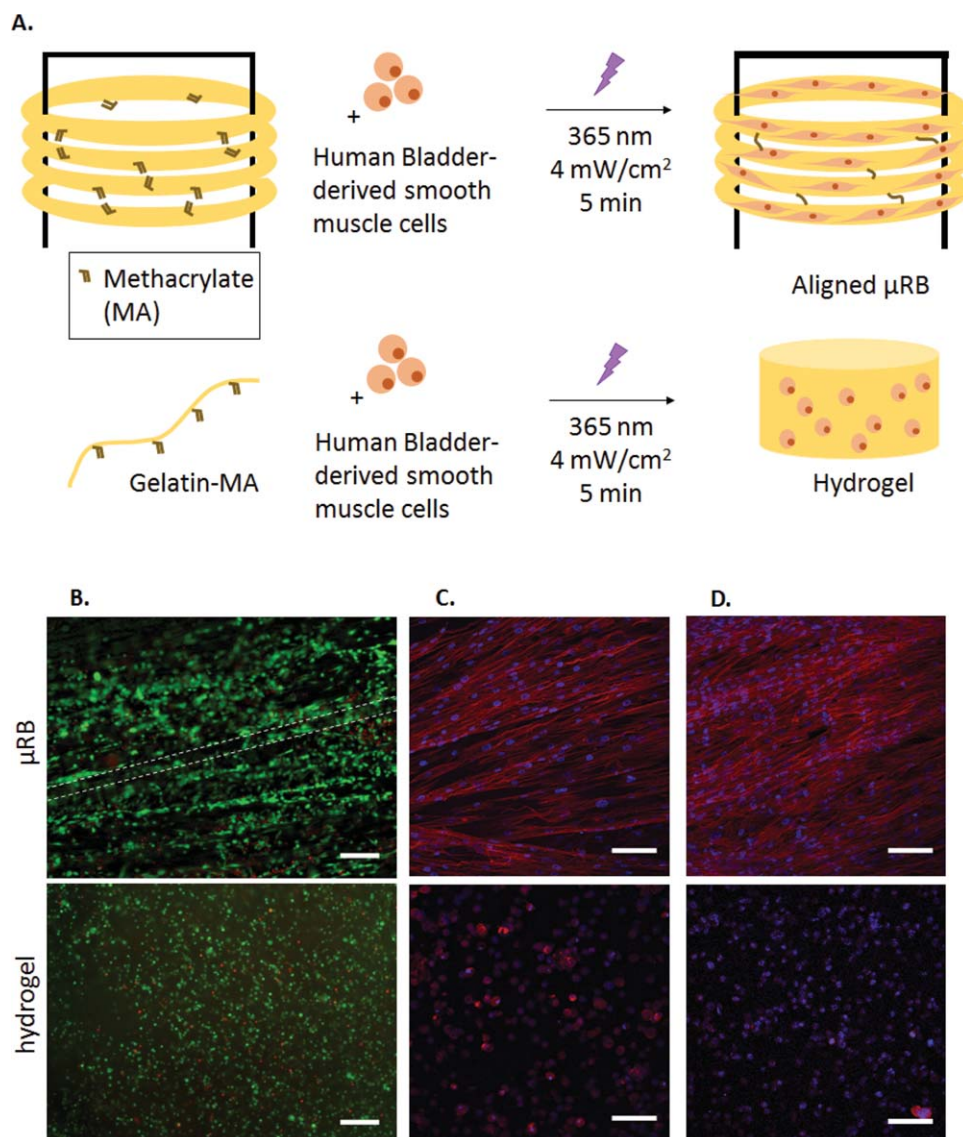


**FIGURE 2.** (A) Schematic of encapsulating cells in 3D scaffolds using either gelatin-based aligned  $\mu$ RBs or conventional gelatin-MA hydrogels. (B) Human smooth muscle cells showed high viability in both aligned  $\mu$ RB scaffolds and gelatin-MA hydrogels (green: live cells, red: dead cells, scale bar: 200  $\mu$ m). Dotted line marks boundary of one individual  $\mu$ RB as an example. (C, D) Aligned  $\mu$ RBs induced fast cell alignment and spreading whereas cells remain round in gelatin-MA hydrogels. (C) At day 7, (D) at day 21 (red: F-actin, blue: nuclei, scale bar: 100  $\mu$ m).

guiding cell alignment in 3D. To repair tissues with aligned structures such as smooth muscle tissues, it is critical to have scaffolds that can guide cell alignment in 3D in a homogeneous manner. However, nano-/micropatterned surfaces are only suitable for generating aligned cell monolayer in 2D manner.<sup>21,22</sup> While the use of cell sheet technology<sup>23</sup> and gel casting method<sup>11</sup> show possibility to assemble aligned cell sheets into multilayer structures, the stacking process of multiple cell sheets is labor-intensive and difficult, and would be inefficient in generating large 3D tissues at a scale, that is, relevant for clinical repair. Furthermore, densely packed cell sheets limit nutrient diffusion, which negatively affects cell survival and engraftment after transplant. Towards moving the cell alignment from 2D to 3D, aligned electrospun fiber scaffolds have been explored to create anisotropic tissues. However, cytotoxic fabrication process of electrospinning only

allows cell seeding after the fabrication, and the nanoporosity within electrospun fiber mesh results in poor cell penetration and heterogeneous cell distribution.<sup>14,15,17</sup> As such, there remains a critical need to develop novel methods to facilitate aligning cells in 3D tissue scale scaffolds.

Here, we report the development of aligned  $\mu$ RB-like hydrogels that can effectively induce cell alignment in 3D with homogeneous cell distribution. Using a wet-spinning process, our method allows rapid and facile fabrication of cm-scale hydrogels with aligned cues, which is a great improvement in scaling up the engineered 3D aligned tissue scale compared with previously reported methods (Fig. 1). Another challenge associated with engineering 3D aligned smooth muscle tissues is the lack of method to achieve homogeneous cell seeding in 3D scaffolds with alignment topography. Conventionally, scaffolds are often formed in a

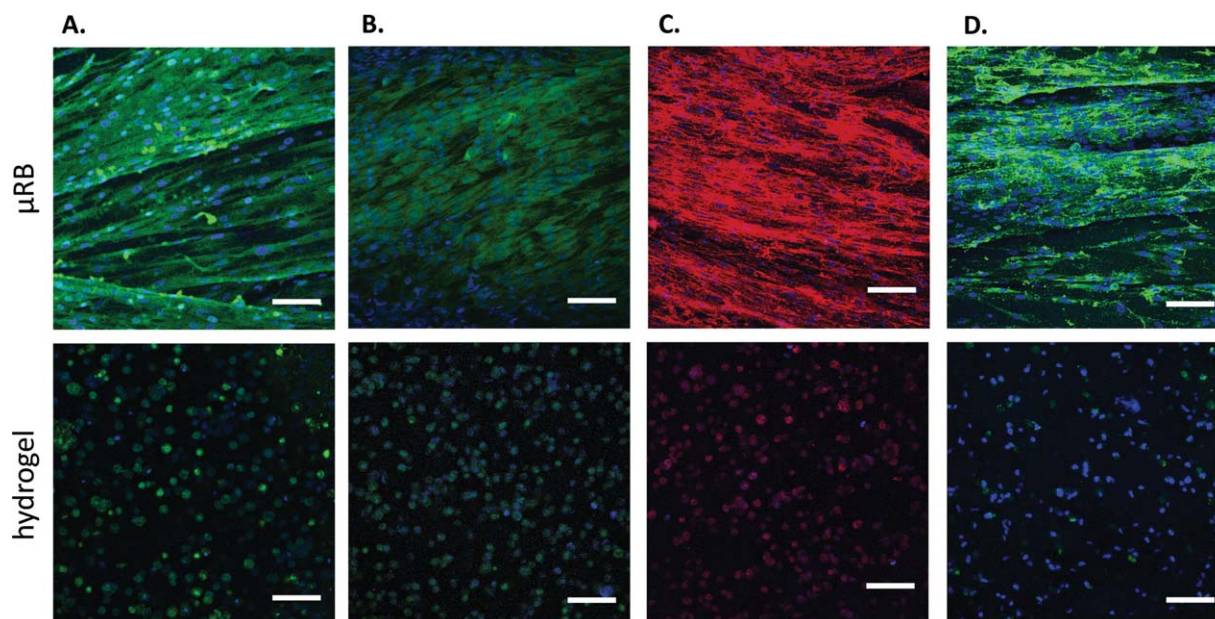


**FIGURE 3.** (A,B) Immunostaining of myosin heavy chain (MHC), a marker of contractile smooth muscle cell phenotype in both aligned  $\mu$ RB scaffolds (top row) and gelatin-MA hydrogels. (A) Day 7, (B) day 21 (green: smooth muscle myosin heavy chain, blue: nuclei, scale bar: 100  $\mu$ m). (C, D) Immunostaining of newly deposited extracellular matrix protein at day 21. (C) Red: collagen I, blue: nuclei, scale bar: 100  $\mu$ m. (D) Green: collagen IV, blue: nuclei, scale bar: 100  $\mu$ m.

one step crosslinking process. As such, if the fabrication process is not cell-friendly, cells can only be seeded postfabrication, which makes it very difficult to achieve uniform cell distribution in 3D. To overcome this challenge, we have designed a two-step crosslinking process for forming cell-laden scaffolds using aligned  $\mu$ RBs. First, aligned  $\mu$ RBs were internally crosslinked to fix the shape of individual  $\mu$ RBs, but they remained uncrosslinked with each other so cells can be mixed homogeneously. After cell-seeding, the scaffold then undergo a secondary crosslinking to form a 3D scaffold (Figs. 1 and 2). Another major advantage of this two-step crosslinking method is that we can achieve macroporosity, which can facilitate nutrient diffusion as well as promote host tissue integration by facilitating cell migration.

Using human smooth muscle as a model cell type, we further confirmed the ability of aligned  $\mu$ RBs to support cell alignment and retention of contractile phenotype in 3D. Smooth muscle myosin heavy chain (MHC) is a contractile marker of smooth muscle cell, and retention of MHC expression is critical for the contractile functions of these cells.<sup>6</sup> Our results showed that aligned  $\mu$ RBs enabled SMCs to maintain MHC expression, confirming the retention of contractile phenotype >3 weeks [Fig. 3(A,B)]. Previously, it was only shown on 2D patterned surface<sup>24,25</sup> that alignment cues can induce matrix deposition following the alignment. Importantly, aligned  $\mu$ RBs guided newly deposited collagen to align in the same direction in 3D, mimicking native ECM organization in smooth muscle tissues. In contrast, conventional gelatin-MA

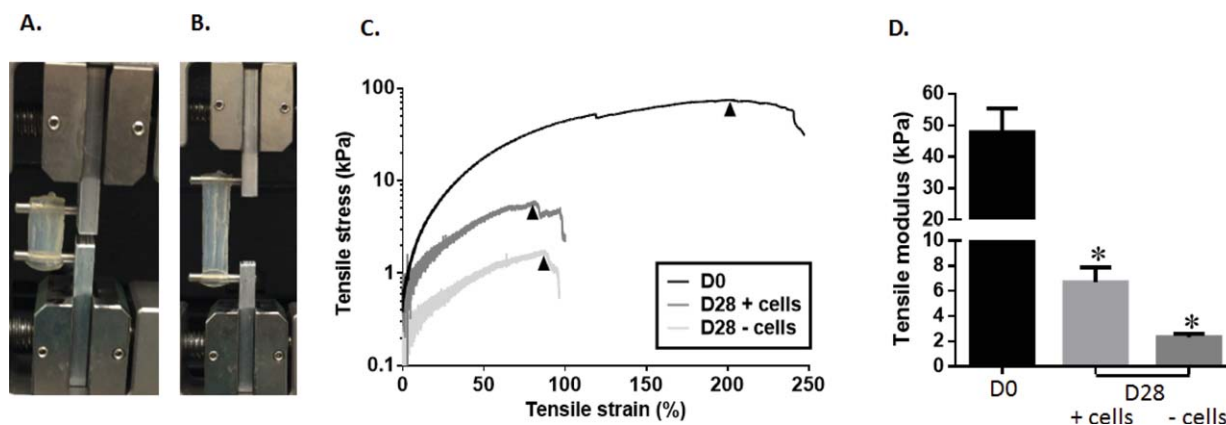


**FIGURE 4.** (A,B) A photograph of aligned  $\mu$ RB scaffold (A) before uniaxial tension test and (B) at maximum tensile strain (200%). (C) Tensile stress-strain curve of aligned  $\mu$ RB scaffold. (D) Calculated tensile modulus from stress-strain curve (\* $p < 0.05$ ).

hydrogel control only allowed pericellular deposition of the proteins due to the nanoporosity and reliance on hydrogel degradation before cells could spread [Fig. 3(C,D)]. Given that cell-ECM interactions play a dynamic role in muscle development and regeneration,<sup>21,26</sup> it is a great advantage that aligned  $\mu$ RBs can guide matrix protein to deposit unidirectionally to better recapitulate the native muscle structures.

Like other tissue types with aligned structures, smooth muscle tissues are characterized by unique tensile property for delivering its contractile functions. Tensile testing showed aligned  $\mu$ RB hydrogels offer good tensile strength (75 kPa) with great stretchability ( $\sim$ 200% strain at maximum tensile stress) (Fig. 4). Previously, electrospun PLGA microfibers were reported to achieve higher tensile strength (1–3 MPa), but less stretchability, with maximum strain before failure limited to 80–137%.<sup>27</sup> Given the much higher water content in  $\mu$ RB hydrogels compared with PLGA microfibers, it is expected that tensile strength would be lower in hydrogels. In fact, the tensile modulus of  $\mu$ RB hydrogels better mimics the range of native muscle tensile modulus (8–15 kPa).<sup>28</sup> Lastly, we observed rapid decrease in tensile strength of acellular  $\mu$ RB scaffolds (from 48 to 2 kPa) using current  $\mu$ RB scaffold formulation (Fig. 4). This rapid loss of tensile strength is likely due to degradation of gelatin  $\mu$ RBs and subsequent decrease in inter-crosslinking among the  $\mu$ RBs. To improve the long-term mechanical support of engineered smooth muscle tissues, future studies could further increase the degree of methacrylation on  $\mu$ RB surface to strengthen intercrosslinking among the  $\mu$ RBs. Importantly, our results showed that tensile modulus of cell-containing  $\mu$ RB groups increased by threefold compared with acellular control, confirming that newly deposited extracellular matrix contribute to the tensile strength of engineered tissues.

## CONCLUSIONS

In sum, here we report a facile method for fabricating gelatin into aligned  $\mu$ RB structures, which guide cell alignment in 3D and allow direct cell encapsulation in tissue scale hydrogels with macroporosity. Aligned  $\mu$ RB hydrogels support high cell viability, fast cell adhesion and spreading, and aligned morphology of human smooth muscles cells  $>28$  days of culture *in vitro*. Smooth muscle cells maintain their mature phenotype, and deposit extracellular matrix proteins along the directions of  $\mu$ RBs, which contributes to enhanced tensile strength of cell-laden hydrogels. We envision that aligned  $\mu$ RBs can provide a novel biomaterials platform for engineering 3D muscle tissues, and may be broadly applicable in engineering other anisotropic tissues with alignment structures including ligaments, tendons, nerves, and blood vessels.

## ACKNOWLEDGMENT

S.L. would also like to thanks Stanford Bio-X fellowship for support.

## REFERENCES

- Owens GK, Kumar MS, Wamhoff BR. Molecular regulation of vascular smooth muscle cell differentiation in development and disease. *Physiol Rev* 2004;84:767–801.
- Amrani Y, Panettieri RA. Airway smooth muscle: contraction and beyond. *Int J Biochem Cell Biol* 2003;35:272–276.
- Bitar KN. Function of gastrointestinal smooth muscle: from signaling to contractile proteins. *Am J Med* 2003;115 Suppl 3A:15S–23S.
- Andersson K-E, Arner A. Urinary bladder contraction and relaxation: Physiology and pathophysiology. *Physiol Rev* 2004;84:935–986.
- Fujii S, Konishi I, Katabuchi H, Okamura H. Ultrastructure of Smooth Muscle Tissue in the Female Reproductive Tract: Uterus and Oviduct. *Ultrastructure of Smooth Muscle*. Berlin: Springer US; 1990. p 197–220.
- Gomez D, Owens GK. Smooth muscle cell phenotypic switching in atherosclerosis. *Cardiovasc Res* 2012;95:156–164.
- Bae JH, Yoo JJ. Cell-based therapy for urinary incontinence. *Kor J Urol* 2010;51:1–7.
- Foubert P, Matrone G, Souttou B, Lere-Dean C, Barateau V, Plouet J, Le Ricousse-Roussanne S, Levy BI, Silvestre JS, Tobelem G. Coadministration of endothelial and smooth muscle progenitor cells enhances the efficiency of proangiogenic cell-based therapy. *Circ Res* 2008;103:751–760.
- Jack GS, Zhang R, Lee M, Xu Y, Wu BM, Rodríguez LV. Urinary bladder smooth muscle engineered from adipose stem cells and a three dimensional synthetic composite. *Biomaterials* 2009;30:3259–3270.
- Shukla D, Box G, Edwards R, Tyson D. Bone marrow stem cells for urologic tissue engineering. *World J Urol* 2008;26:341–349.
- Jiao A, Tropper NE, Yang HS, Kim J, Tsui JH, Frankel SD, Murry CE, Kim DH. Thermoresponsive nanofabricated substratum for the engineering of three-dimensional tissues with layer-by-layer architectural control. *ACS Nano* 2014;8:4430–4439.
- Hwang CM, Park Y, Park JY, Lee K, Sun K, Khademhosseini A, Lee SH. Controlled cellular orientation on PLGA microfibers with defined diameters. *Biomed Microdevices* 2009;11:739–746.
- Chew SY, Mi R, Hoke A, Leong KW. The effect of the alignment of electrospun fibrous scaffolds on Schwann cell maturation. *Biomaterials* 2008;29:653–661.
- Zhou Q, Xie J, Bao M, Yuan H, Ye Z, Lou X, Zhang Y. Engineering aligned electrospun PLLA microfibers with nano-porous surface nanotopography for modulating the responses of vascular smooth muscle cells. *J Mater Chem B* 2015;3:4439–4450.
- Murray-Dunning C, McArthur S, Sun T, McKean R, Ryan A, Haycock J. Three-dimensional alignment of Schwann cells using hydrolysable microfiber scaffolds: Strategies for peripheral nerve repair. In: Haycock JW, editor. *3D Cell Culture*. Humana Press; 2011. p 155–166.
- Kawamura M, Miyagawa S, Fukushima S, Saito A, Miki K, Ito E, Sougawa N, Kawamura T, Daimon T, Shimizu T, Okano T, Toda K, Sawa Y. Enhanced survival of transplanted human induced pluripotent stem cell-derived cardiomyocytes by the combination of cell sheets with the pedicled omental flap technique in a porcine heart. *Circulation* 2013;128(11 Suppl 1):S87–S94.
- An J, Chua CK, Leong KF, Chen CH, Chen JP. Solvent-free fabrication of three dimensionally aligned polycaprolactone microfibers for engineering of anisotropic tissues. *Biomed Microdevices* 2012;14:863–872.
- Han L-H, Yu S, Wang T, Behn AW, Yang F. Microribbon-like elastomers for fabricating macroporous and highly flexible scaffolds that support cell proliferation in 3D. *Adv Funct Mater* 2013;23:346–358.
- Han L-H, Lai JH, Yu S, Yang F. Dynamic tissue engineering scaffolds with stimuli-responsive macroporosity formation. *Biomaterials* 2013;34:4251–4258.
- Sutter M, Siepmann J, Hennink WE, Jiskoot W. Recombinant gelatin hydrogels for the sustained release of proteins. *J Control Release* 2007;119:301–312.
- Kim DH, Lipke EA, Kim P, Cheong R, Thompson S, Delannoy M, Suh KY, Tung L, Levchenko A. Nanoscale cues regulate the structure and function of macroscopic cardiac tissue constructs. *Proc Natl Acad Sci USA* 2010;107:565–570.
- McDevitt TC, Angello JC, Whitney ML, Reinecke H, Hauschka SD, Murry CE, Stayton PS. *In vitro* generation of differentiated cardiac myofibers on micropatterned laminin surfaces. *J Biomed Mater Res* 2002;60:472–479.
- Okano T, Yamada N, Sakai H, Sakurai Y. A novel recovery-system for cultured-cells using plasma-treated polystyrene dishes grafted with poly(*N*-isopropylacrylamide). *J Biomed Mater Res* 1993;27:1243–1251.

24. Wang JHC, Jia F, Gilbert TW, Woo SLY. Cell orientation determines the alignment of cell-produced collagenous matrix. *J Biomech* 2003; 36:97–102.
25. Manwaring ME, Walsh JF, Tresco PA. Contact guidance induced organization of extracellular matrix. *Biomaterials* 2004;25:3631–3638.
26. Hinds S, Bian W, Dennis RG, Bursac N. The role of extracellular matrix composition in structure and function of bioengineered skeletal muscle. *Biomaterials* 2011;32:3575–3583.
27. Masoumi N, Larson BL, Annabi N, Kharaziha M, Zamanian B, Shapero KS, Cubberley AT, Camci-Unal G, Manning KB, Mayer JE. Jr., Khademhosseini A. Electrospun PGS:PCL microfibers align human valvular interstitial cells and provide tunable scaffold anisotropy. *Adv Health Mater* 2014;3:929–939.
28. Engler AJ, Griffin MA, Sen S, Bonnemann CG, Sweeney HL, Discher DE. Myotubes differentiate optimally on substrates with tissue-like stiffness: Pathological implications for soft or stiff microenvironments. *J Cell Biol* 2004;166:877–887.